Solving Doppler-Angle Ambiguity of BPSK-MIMO FMCW Radar System

JAEHOON JUNG[1], (Graduate Student Member, IEEE),
SOHEE LIM[1], (Graduate Student Member, IEEE),
SEONG-CHEOL KIM[1], (Senior Member, IEEE),
AND SEONGWOOK LEE[2], (Member, IEEE)

[1]Department of Electrical and Computer Engineering, College of Engineering, Institute of New Media and Communications,
Seoul National University, Seoul 08826, Republic of Korea
[2]School of Electronics and Information Engineering, College of Engineering, Korea Aerospace University, Gyeonggi-do 10540, Republic of Korea

Corresponding author: Seongwook Lee (swl90@kau.ac.kr)

ABSTRACT In a multiple-input multiple-output (MIMO) radar system, binary phase-shift keying (BPSK) modulation is widely used to separate signals transmitted from multiple transmit (Tx) antennas. However, when the BPSK modulation is applied to the frequency-modulated continuous-wave (FMCW) radar system, there is an occurrence of Doppler-angle ambiguity due to the properties of the modulation scheme. In other words, the maximum detectable velocity is reduced in proportion to the number of Tx antennas, and the angle estimation performance can be degraded when a moving target induces a Doppler phase shift. Therefore, in this paper, we propose a method for solving the Doppler-angle ambiguity in the BPSK-MIMO FMCW radar system. The proposed method involves comparing and arranging the phases of signals corresponding to the same target in the range-velocity detection results. By arranging the phases to form an arithmetic sequence, the signals from each Tx antenna can be distinguished and the unambiguous velocity and angle of the target can be estimated. In addition, by using a general phase-shift keying (PSK) modulation scheme, the proposed method can be applied to an arbitrary MIMO system regardless of the number of Tx antennas.

INDEX TERMS Binary phase-shift keying, Doppler-angle ambiguity, frequency-modulated continuous-wave, multiple-input multiple-output.

I. INTRODUCTION

Frequency-modulated continuous-wave (FMCW) radars are widely used as automotive sensors to obtain information about a surrounding target such as its range, velocity, and angle. In addition, the multiple-input multiple-output (MIMO) antenna system is being utilized to obtain high angular resolution with a limited hardware size [1]. In the MIMO FMCW radar system, the signals transmitted from multiple transmit (Tx) antennas are required to be separated at the receiving (Rx) antenna end [2], [3]. Various multiplexing methods, such as time-division multiplexing (TDM) [4], [5], frequency-division multiplexing (FDM) [6], [7], and

The associate editor coordinating the review of this manuscript and approving it for publication was Cheng Hu.

code-division multiplexing (CDM) [8], [9], can be used to maintain the orthogonality of the transmitted signals.

Among these multiplexing schemes, the TDM-based method is the most widely used due to its ease of implementation. However, the main drawback of the TDM-based method is that the maximum detectable velocity decreases in proportion to the number of Tx antennas due to its extended chirp repetition time [10]. In addition, since each Tx antenna transmits a signal alternately, the Doppler effect caused by the movement of the target can degrade the angle estimation performance [11], [12]. To address these issues, several studies have attempted to solve the Doppler-angle ambiguity of the TDM-MIMO radar system [13], [14]. In [13], the conventional chirp sequence was modified to assign a different starting frequency for each chirp. Similarly, in [14], multiple chirp repetition frequencies were assigned and the

original maximum detectable velocity was recovered using the Chinese remainder theorem. However, a major drawback associated to these methods is that the existing hardware has to be modified.

Another approach is to assign specific codes to each Tx antenna and transmitting the signals simultaneously. In particular, a binary phase-shift keying (BPSK) method is widely used in which the phase of the transmitted signal is modulated by 0 or π [15]. In this method, the signals from each Tx antenna can be separated using the orthogonality of the transmitted signals. Unlike the TDM-MIMO system, the BPSK-MIMO system requires an additional decoding process to separate signals from each Tx antennas. However, it can achieve a higher signal-to-noise ratio (SNR) using the complete transmission capabilities of the Tx antennas [16].

The BPSK-MIMO system also suffers from Doppler-angle ambiguity because the block time used for velocity estimation is extended in proportion to the number of Tx antennas. In [17], multiple frames with different unambiguous velocity was used and the original maximum detectable velocity was recovered using the Chinese remainder theorem or clustering algorithm. However, this method requires the existing hardware to be modified similar to the methods used in [13] and [14]. The authors in [17] also attempted to retrieve the original maximum detectable velocity by compensating the phase of the received signals using the estimated velocity value. However, this method of directly correcting the phase is highly unstable because a small error in the estimated velocity value can result in large errors.

Therefore, in this paper, we propose an efficient method for solving Doppler-angle ambiguity in the BPSK-MIMO radar system. The range-velocity detection results of the BPSK-MIMO radar system reveals that a target is duplicated as many times as the number of Tx antennas. In other words, one real target and multiple ghost targets are detected. To distinguish the real target from ghost targets, we use the idea that the phase values of signals corresponding to those of real and ghost targets should have the form of an arithmetic sequence. Thus, by correctly arranging these phase values, we can determine from which Tx antenna each target is generated. After identifying the real target, the unambiguous velocity of the target can be estimated and angle estimation can also be performed simultaneously by using the arranged phase values.

The contribution of our work can be summarized as follows. Through the proposed method, we can overcome the problem of reduced maximum detectable velocity even when multiple Tx antennas are used. In addition, unlike the TDM-based method in which the signals are received alternately, the proposed method uses signals received simultaneously. As a result, we can mitigate the inaccuracy of angle estimation due to the movement of the target between different time slots. Moreover, the proposed method does not require additional hardware and can be implemented in the existing digital signal processor of the radar system. This is because two-dimensional (2D) fast Fourier transform (FFT)

for the range-velocity estimation is an essential signal processing that should be performed in the FMCW radar system, and only an algorithm that arranges the phase values needs to be additionally implemented.

The remainder of this paper is organized as follows. In Section II, the fundamentals of the BPSK-MIMO FMCW radar system are introduced. Then, conventional signal processing methods for the radar system and their problems are presented in Section III. Next, a method to solve the Doppler-angle ambiguity is proposed in Section IV. Finally, we conclude this paper in Section V.

II. BPSK-MIMO FMCW RADAR SYSTEM
A. FUNDAMENTALS OF FMCW RADAR
The FMCW radar transmits a periodic chirp signal whose angular frequency increases linearly with time. The transmitted signal for a single chirp can be expressed as

$$s(t) = \exp\left\{ j2\pi\left(f_c t + \frac{B}{2T_c}t^2 \right) \right\} \quad (0 \le t \le T_c), \quad (1)$$

where f_c, B, and T_c denote the carrier frequency, bandwidth, and duration of the chirp signal, respectively. As shown in Fig. 1, the transmission is repeated for L consecutive chirps. Then, the received signals are conjugately mixed with the transmitted signal to eliminate the carrier frequency component. The resulting intermediate frequency (IF) band signal can be expressed as a 2D exponential function:

$$x[n, \, l] = \exp\left\{ j2\pi\left(\frac{2BR}{T_c c}nT_s + \frac{2v}{\lambda}lT_c + \phi \right) \right\}$$
$$(n = 0, \, 1, \, \cdots, \, N - 1)$$
$$(l = 0, \, 1, \, \cdots, \, L - 1). \quad (2)$$
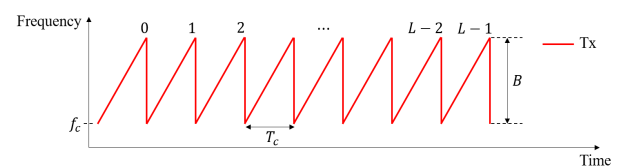

FIGURE 1. Transmitted waveform of the FMCW radar.

The two indices n and l represent the sampling index within each chirp and the chirp index, respectively. In addition, R and v denote the range and velocity of the target, T_s is the sampling period, λ is the wavelength of transmitted signal, and ϕ is the constant phase component. This IF band signal has frequencies of $\frac{2BR}{T_c c}$ and $\frac{2v}{\lambda}$ along the n-axis and l-axis, respectively. Therefore, by applying the 2D Fourier transform to (2), the range and velocity of the target can be estimated.

Moreover, the estimation of angle can be achieved using a uniform linear array (ULA) antenna system, as shown in Fig. 2. When the antenna spacing is d and incident angle of the received signal is θ, the phase difference between adjacent antennas can be expressed as $\omega = 2\pi\frac{d\sin\theta}{\lambda}$. This phase term can be incorporated into (2) to produce a three-dimensional
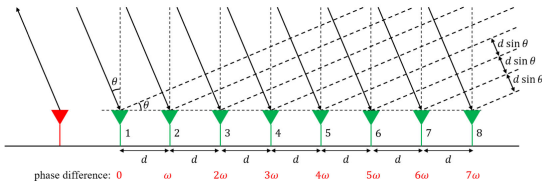
FIGURE 2. Angle estimation using ULA antenna system (1 Tx antenna, 8 Rx antennas).

IF band signal, which can be expressed as

$$
\begin{aligned}
x[n, l, p] = \exp \Big\{ j2\pi \Big(& \frac{2BR}{T_c c} n T_s + \frac{2v}{\lambda} l T_c \\
& + \frac{d \sin \theta}{\lambda} p + \phi \Big) \Big\}
\end{aligned}
$$
$$(n = 0, 1, \cdots, N - 1)$$
$$(l = 0, 1, \cdots, L - 1)$$
$$(p = 0, 1, \cdots, P - 1), \qquad (3)$$

where p is the antenna index and P is the number of Rx antennas. This signal is commonly known as radar data cube in the literature. By applying Fourier transform to each dimension of the radar data cube, the range, velocity, and angle of the target can be estimated.

B. BPSK-MIMO FMCW RADAR

In a MIMO radar system, multiple Tx and Rx antennas are used to improve the detection performance of the radar. For example, Fig. 3 shows a MIMO radar system with two Tx antennas and four Rx antennas. Since the signal transmitted from Tx 2 travels an additional distance of $4d \sin \theta$, the phase of the received signal that was transmitted by Tx 2 is $2\pi \frac{4d \sin \theta}{\lambda}$ higher than that transmitted by Tx 1. As a result, the angle estimation performance of the antenna configuration shown in Fig. 3 is similar to that of the one shown in Fig. 2. The main advantage of the MIMO antenna scheme is that the total number of antenna elements can be reduced.
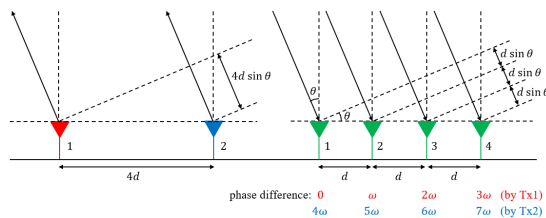

FIGURE 3. Angle estimation using MIMO ULA antenna system (2 Tx antennas, 4 Rx antennas).

To fully utilize the MIMO antenna system, we have to differentiate the signals transmitted from different Tx antennas. For example, for the case of Fig. 3, it is necessary to distinguish which received signal component is transmitted from Tx 1 and which signal component is transmitted

from Tx 2. There are various multiplexing schemes to solve this problem, such as TDM, FDM, and CDM. Among these various techniques, BPSK is a method of modulating the phase of the transmit signal using a preassigned code. The code is specially designed to make the transmitted signals orthogonal to each other.

Fig. 4 shows the transmitted signals of BPSK-MIMO radar when two Tx antennas are used. When a chirp is assigned with a code of 1, the phase of the transmit signal is modulated by 0, which means that the signal

$$
\begin{aligned}
s(t) \exp(j0) &= s(t) \\
&= \exp \Big\{ j2\pi \Big(f_c t + \frac{B}{2T_c} t^2 \Big) \Big\} \qquad (4)
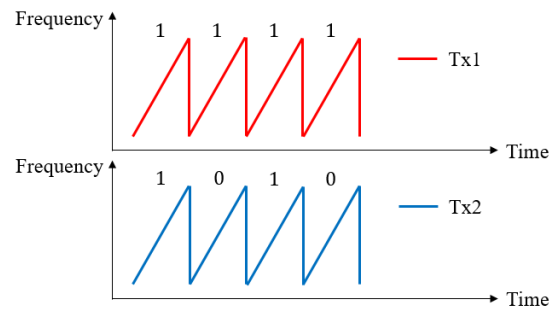\end{aligned}
$$

FIGURE 4. Transmitted signals of BPSK-MIMO radar system (2 Tx antennas).

is transmitted. On the other hand, if the chirp is assigned with a code of 0, the phase of the transmit signal is modulated by π, and the signal

$$
\begin{aligned}
s(t) \exp(j\pi) &= -s(t) \\
&= - \exp \Big\{ j2\pi \Big(f_c t + \frac{B}{2T_c} t^2 \Big) \Big\} \qquad (5)
\end{aligned}
$$

is transmitted. As shown in Fig. 4, when Tx 1 transmits with a code of $1111 \cdots$ and Tx 2 transmits with a code of $1010 \cdots$, the received signal of the odd index can be expressed as $r_{odd}(t) = r_1(t) + r_2(t)$ and that of the even index can be expressed as $r_{even}(t) = r_1(t) - r_2(t)$. Here, $r_1(t)$ and $r_2(t)$ represent the received signal component from Tx 1 and Tx 2. Therefore, received signals from each Tx antenna can be decomposed by the following decoding process:

$$r_1(t) = \frac{1}{2} \{ r_{odd}(t) + r_{even}(t) \} \qquad (6)$$

$$r_2(t) = \frac{1}{2} \{ r_{odd}(t) - r_{even}(t) \} \qquad (7)$$

III. TARGET DETECTION VIA CONVENTIONAL RADAR SIGNAL PROCESSING

This section illustrates target detection using a BPSK-MIMO radar via conventional processing techniques. The detection of targets using radar mainly involves estimating the range, velocity, and angle of targets, as explained in Section II-A. In the BPSK-MIMO radar system, the range estimation

is performed in a similar manner to that in a general FMCW radar system. However, when the conventional velocity and angle estimation method is used, problems arise due to the Doppler-angle ambiguity of the MIMO system. The velocity estimation method and related issues concerning the BPSK-MIMO radar system will be explained in Section III-A, followed by the issues related to angle estimation in Section III-B.

A. VELOCITY ESTIMATION USING BPSK-MIMO RADAR SYSTEM

In a FMCW radar system, velocity estimation is performed using the phase difference between multiple chirp signals. For example, in a conventional FMCW radar system, the phase differs by $2\pi\frac{2v}{\lambda}T_c$ between adjacent chirps, as observed from (2) and (3), and the velocity is estimated using the phase increment among multiple chirp signals. However, in a BPSK-MIMO radar system, the received signal consists of multiple signal components from multiple Tx antennas, and the phase increment cannot be simply expressed as $2\pi\frac{2v}{\lambda}T_c$. Fig. 5 shows the received signals of Rx 1 when the antenna configuration is set as shown in Fig. 3 and the transmitted signals are modulated as shown in Fig. 4. The first term denotes the general received signal with a phase increment of $2\pi\frac{2v}{\lambda}T_c$. However, the second term includes a sign reversal, so the phase increases by $2\pi\frac{2v}{\lambda}T_c+\pi$. As a result, two peaks occur when 2D Fourier transform is applied to the IF band signal.

$$\begin{bmatrix} r_A(t) = \exp\left\{j2\pi\left(\frac{2BR}{T_cc}t\right)\right\} & + \exp\left\{j2\pi\left(\frac{2BR}{T_cc}t+\frac{4d\sin\theta}{\lambda}\right)\right\} \\ r_B(t) = \exp\left\{j2\pi\left(\frac{2BR}{T_cc}t+\frac{2v}{\lambda}T_c\right)\right\} & - \exp\left\{j2\pi\left(\frac{2BR}{T_cc}t+\frac{2v}{\lambda}T_c+\frac{4d\sin\theta}{\lambda}\right)\right\} \\ r_C(t) = \exp\left\{j2\pi\left(\frac{2BR}{T_cc}t+\frac{2v}{\lambda}2T_c\right)\right\} & + \exp\left\{j2\pi\left(\frac{2BR}{T_cc}t+\frac{2v}{\lambda}2T_c+\frac{4d\sin\theta}{\lambda}\right)\right\} \\ r_D(t) = \exp\left\{j2\pi\left(\frac{2BR}{T_cc}t+\frac{2v}{\lambda}3T_c\right)\right\} & - \exp\left\{j2\pi\left(\frac{2BR}{T_cc}t+\frac{2v}{\lambda}3T_c+\frac{4d\sin\theta}{\lambda}\right)\right\} \end{bmatrix}$$

Signal from Tx 1   **Signal from Tx 2**
$r_1(t)$ $r_2(t)$

Phase increases   Phase increases
by $2\pi\frac{2v}{\lambda}T_c$ by $2\pi\frac{2v}{\lambda}T_c+\pi$

FIGURE 5. Received signals of BPSK-MIMO radar system (2 Tx antennas).

We performed a simulation using the aforementioned antenna configuration, assuming that three targets are moving in the field of view of the radar. The result of range-velocity estimation is shown in Fig. 6. The simulation parameters were set according to Table 1, where conventional parameters for automotive radar were used [18]. This resulted in a maximum detectable velocity of $\pm\frac{\lambda}{4T_c}=\pm19.48$ m/s [19]. In addition, the SNR was set as 0 dB and the range and velocity of the targets were set as (30 m, 12 m/s), (50 m, 4 m/s), and (60 m, −3 m/s), respectively. It can be observed from the figure that two peaks occurred for each target, resulting in Doppler ambiguity. This is because one peak is generated due to signal from Tx 1 and the other peak is generated due to
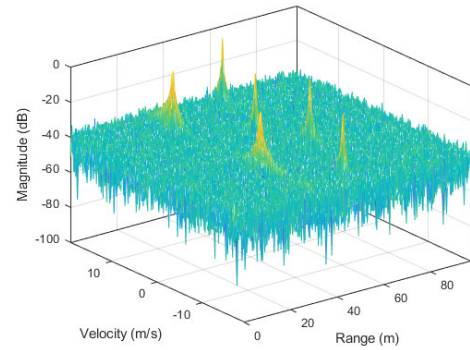

FIGURE 6. Range-velocity estimation using BPSK-MIMO radar system (2 Tx antennas).

TABLE 1. Specifications of the radar system.

Parameter	Value
Modulation scheme	FMCW
Number of Tx antennas	2
Number of Rx antennas	4
Center frequency, f_c	77 GHz
Bandwidth, B	1 GHz
Chirp duration, T_c	50 μs
Number of samples per chirp, N	256
Number of chirps, L	128
Sampling period, T_s	0.07 μs

signal from Tx 2. For example, for the target located at 30 m, one peak occurred at 12 m/s due to the signal from Tx 1 and another peak occurred at $12-19.48=-7.48$ m/s due to the signal from Tx 2. Similar results were observed for all targets and the velocities of the targets were not uniquely determined. As a result, the maximum detectable velocity was reduced by half, from ±19.48 m/s to ±9.74 m/s.

The results can be extended to BPSK-MIMO radar systems that consist of more than two Tx antennas. Fig. 7 shows the simulation result when four Tx antennas are used instead of two Tx antennas. Excluding the number of Tx antennas, the radar system parameters and target information were set the same as in Fig. 6. Moreover, the phase of the signals transmitted from four Tx antennas were coded using the Hadamard coding method. In this method, four Tx antennas transmit with a code of (1, 1, 1, 1), (1, 0, 1, 0), (1, 1, 0, 0), and (1, 0, 0, 1). Then, the received signals from each Tx antenna are decomposed using the orthogonality between the codes [20]. As shown in the figure, four peaks occurred for each target, and the maximum detectable velocity was reduced by a quarter. In general, when multiplexing is performed by dividing time slots, the maximum detectable velocity reduces by the number of Tx antennas. This can considerably degrade the velocity estimation performance, making it undesirable for automotive applications. Therefore, it is necessary to determine the correspondence between peaks and Tx antennas to solve Doppler ambiguity and maintain the maximum detectable velocity.
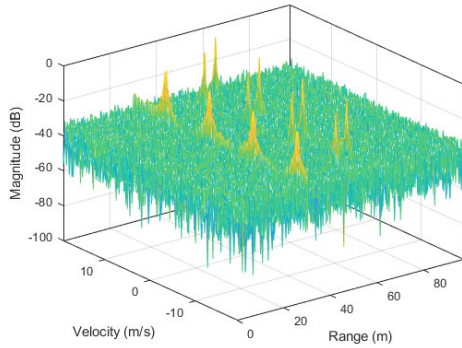
FIGURE 7. Range-velocity estimation using BPSK-MIMO radar system (4 Tx antennas).

B. ANGLE ESTIMATION USING BPSK-MIMO RADAR SYSTEM

In a MIMO radar system, the signal from each Tx antenna needs to be separated when estimating the angle of targets, as explained in Section II-B. For this purpose, a decoding process in (6) and (7) is applied to the received signals in a BPSK-MIMO radar system. However, when the targets are non-stationary, the signals from each Tx antenna cannot be separated properly due to the velocity-induced phase term. For example, when the decoding process is applied to the received signals shown in Fig. 5, the resulting signals are

$$r_1(t) = \frac{1}{2}\{r_A(t) + r_B(t)\}$$
$$\neq \exp\left\{j2\pi\left(\frac{2BR}{T_c c}t\right)\right\} \qquad (8)$$

and

$$r_2(t) = \frac{1}{2}\{r_A(t) - r_B(t)\}$$
$$\neq \exp\left\{j2\pi\left(\frac{2BR}{T_c c}t + \frac{4d\sin\theta}{\lambda}\right)\right\}. \qquad (9)$$

Due to the velocity-induced phase term $2\pi\frac{2v}{\lambda}T_c$, the unnecessary components do not cancel out and signals from each Tx antenna cannot be separated properly. Fig. 8 shows the angle estimation results for the case of stationary target and non-stationary target. The angle was equally set as $-20°$, and the velocity was set as 0 m/s and 15 m/s, respectively. As shown in the figure, the angle of the target was properly estimated when the target is stationary. There was a minor error in the estimated angle because we used the FFT method for angle estimation. The estimation accuracy can be improved using more complex algorithms such as MUSIC [21] or ESPRIT [22], but we used the FFT method for fast computation. Conversely, when the target is non-stationary, there was a large error in estimating the angle of target.

To solve this problem, the phase of the received signal can be compensated to eliminate the velocity-induced phase term, either in time-domain [11] or frequency-domain [17]. In [11] and [17], the velocities of the targets were estimated first, and
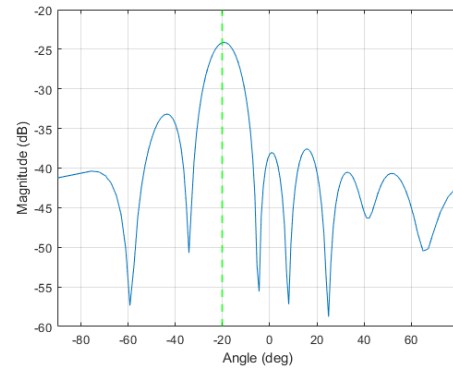
(a)
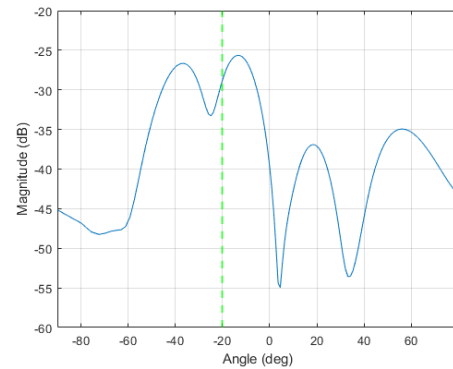
(b)

FIGURE 8. Angle estimation using BPSK-MIMO radar system: (a) stationary target (b) non-stationary target.

then the estimated velocity value was used to compensate the phase of the received signal by $-\frac{2v}{\lambda}T_c$. However, these phase compensation methods can result in large errors even when the estimated velocity value is slightly different from the true value. For example, when the velocity resolution is v_{res}, the velocity bin is divided into intervals of v_{res} and the estimated velocity can deviate from the true value by $\frac{v_{res}}{2}$ regardless of noise. The velocity resolution is defined as $\frac{\lambda}{2LT_c}$ in the FMCW radar system [19]. Hence, the compensated phase value can be offset by $\frac{2v}{\lambda}T_c = \frac{1}{2L}$. Since this value is in similar order with $\frac{d\sin\theta}{\lambda}$, the angle of targets cannot be reliably estimated even when phase compensation is applied.

IV. PROPOSED METHOD FOR SOLVING DOPPLER-ANGLE AMBIGUITY
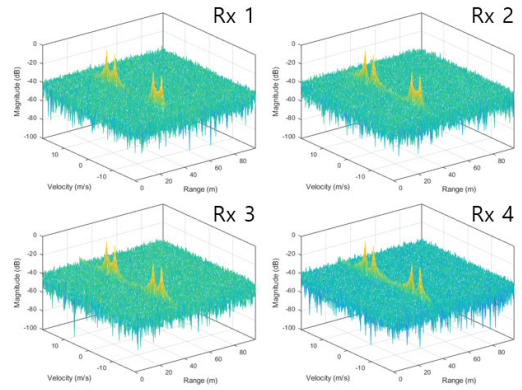### A. PROPOSED METHOD AND PERFORMANCE EVALUATION

In this section, we propose an efficient method of distinguishing the signals from each Tx antenna to solve the aforementioned problems when estimating the velocity and angle of targets. To distinguish the signals from each Tx antenna, we note that the phase of the received signals forms an arithmetic progression, as illustrated in Fig. 3. If the signal transmitted by Tx 1 and received by Rx 1 results in a phase of ϕ, the phase of the other received signals can be
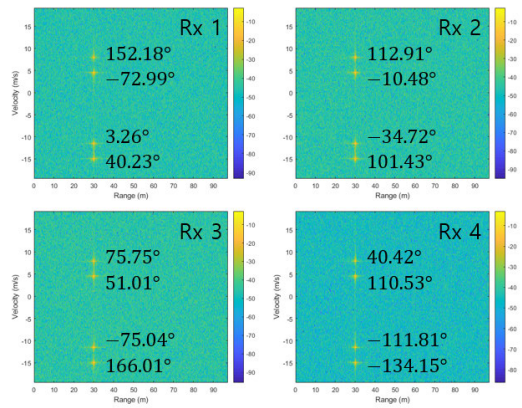
expressed as

$$Tx\ 1 \rightarrow Rx\ 1 : \phi$$
$$Tx\ 1 \rightarrow Rx\ 2 : \phi + \omega$$
$$Tx\ 1 \rightarrow Rx\ 3 : \phi + 2\omega$$
$$Tx\ 1 \rightarrow Rx\ 4 : \phi + 3\omega$$
$$Tx\ 2 \rightarrow Rx\ 1 : \phi + 4\omega$$
$$Tx\ 2 \rightarrow Rx\ 2 : \phi + 5\omega$$
$$Tx\ 2 \rightarrow Rx\ 3 : \phi + 6\omega$$
$$Tx\ 2 \rightarrow Rx\ 4 : \phi + 7\omega, \tag{10}$$

which forms an arithmetic sequence. In particular, when two received signal sequences from two Tx antennas are arranged to form an arithmetic progression, the former sequence should correspond to the signal from Tx 1 and the latter should correspond to Tx 2. This phase information will be utilized to determine the correspondence between signals and Tx antennas.

The overall procedure of applying the proposed method is shown in Fig. 9. First, we apply the 2D FFT to the IF band signal received at each Rx antenna. Through this process, we obtain a range-velocity detection result where each target is duplicated due to the properties of BPSK modulation. Then, we apply the constant false alarm rate (CFAR) algorithm to extract the peak values of each target and record the phase of these peak values [23]. By arranging these phase values to form an arithmetic sequence, we can determine which peak corresponds to which Tx antenna. Specifically, the first sequence should belong to the signal from Tx 1, and the second sequence should belong to the signal from Tx 2. After the signals from each Tx antenna are separated, we can apply the velocity and angle estimation algorithm to obtain an unambiguous estimation result.
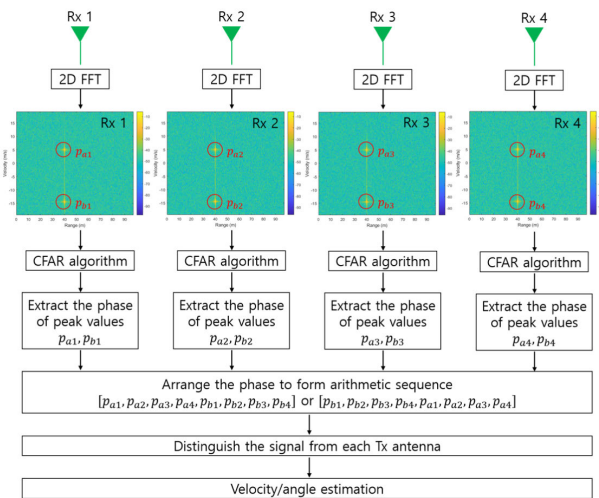
FIGURE 9. Proposed method of solving Doppler-angle ambiguity.

Fig. 10 shows an example of solving Doppler-angle ambiguity using the proposed method. The simulation parameters

FIGURE 10. Range-velocity estimation results of each Rx antenna (2 Tx antennas and 4 Rx antennas): (a) 3D view (b) 2D view from the top.

were set according to Table 1 with two Tx antennas and four Rx antennas. To demonstrate that the proposed method can be applied when there are multiple targets in the same range bin, the range, velocity, and angle of targets were set as (30 m, −15 m/s, 20°) and (30 m, 8 m/s, −12°), respectively. As shown in the figure, two peaks occurred for each target, resulting in a total of four peaks. Because the Doppler ambiguity results in another peak shifted by half of the maximum detectable velocity, we can determine that (30 m, −15 m/s) and (30 m, 4.48 m/s) are due to the same target and (30 m, −11.48 m/s) and (30 m, 8 m/s) are due to another target. As a result, we can resolve the Doppler ambiguity of two targets separately.

First, we investigate whether the target's true velocity is −15 m/s or 4.48 m/s. The phase sequence corresponding to the peak location (30 m, −15 m/s) was $\boldsymbol{p_a} = [40.23°$ $101.43°\ 166.01°\ −134.15°]$ and those corresponding to the peak location (30 m, 4.48 m/s) was $\boldsymbol{p_b} = [−72.99°\ −10.48°$ $51.01°\ 110.53°]$, respectively. By arranging these two phase sequences, we note that the cascaded sequence $[\boldsymbol{p_a}\ \boldsymbol{p_b}]$ forms an arithmetic progression. Thus, we can decide that $\boldsymbol{p_a}$ corresponds to the signal from Tx 1 and $\boldsymbol{p_b}$ corresponds to the signal from Tx 2. Furthermore, we note that the signal from Tx 1 is a general FMCW signal and that from Tx 2 is

a sign-reversing FMCW signal, as discussed in Figs. 4 and 5. Therefore, we can conclude that −15 m/s represents the true velocity of the target and 4.48 m/s corresponds to ghost target that resulted from the sign reversal of Tx 2. By distinguishing the signal from each Tx antenna, the Doppler ambiguity was resolved and the velocity of the target was uniquely determined without reducing the maximum detectable velocity by half.

Next, we repeat the same process to determine whether the target's true velocity is −11.48 m/s or 8 m/s. The phase sequence corresponding to the peak location (30 m, −11.48 m/s) was $p_c = [3.26°\ -34.72°\ -75.04°\ -111.81°]$ and those corresponding to the peak location (30 m, 4.48 m/s) was $p_d = [152.18°\ 112.91°\ 75.75°\ 40.42°]$, respectively. Because the cascaded sequence $[p_d\ p_c]$ forms an arithmetic progression, we can decide that p_d corresponds to the signal from Tx 1 and the target's true velocity is 8 m/s. Fig. 11 shows the unwrapped phase values of eight virtual antennas, which corresponds to $[p_a\ p_b]$ and $[p_d\ p_c]$. The phase values were unwrapped to prevent discontinuity by making the difference between consecutive phase values less than 180°. It is clear from the figure that correctly cascaded phase sequence forms an arithmetic progression.
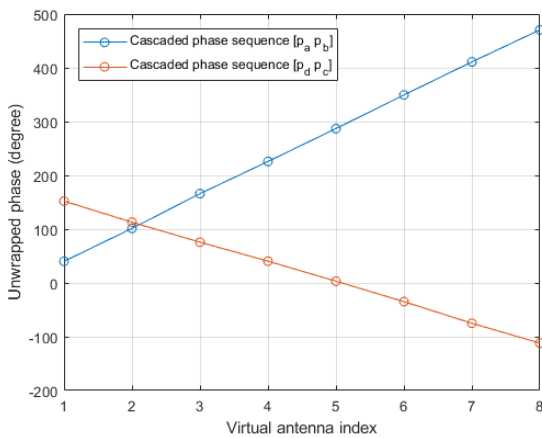
FIGURE 11. Unwrapped phase values of virtual antennas.

The angle estimation can also be performed simultaneously using the arranged phase sequences. There are no such issues as non-stationary targets or phase compensation because signals from each Tx antenna are separated. For example, the angle of the target corresponding to (30 m, −15 m/s) can be estimated by applying the FFT to the sequence $[p_a\ p_b]$. Likewise, the angle of the target corresponding to (30 m, 8 m/s) can be estimated by applying the FFT to the sequence $[p_d\ p_c]$. The results of angle estimation are shown in Fig. 12. As shown in the figure, two target information were resolved and the angles of 20° and −12° were correctly estimated.

In addition, we analyzed the performance of the proposed method by varying the SNR. Fig. 13 shows the unwrapped phase values of eight virtual antennas for various SNRs.
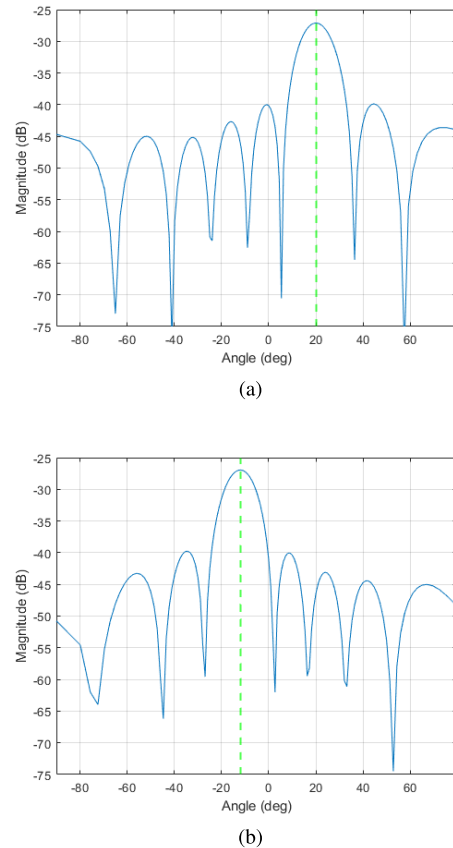

FIGURE 12. Angle estimation results: (a) target corresponding to (30 m, −15 m/s) (b) target corresponding to (30 m, 8 m/s).
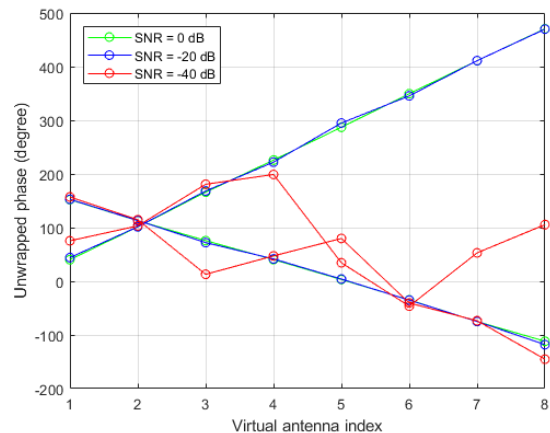

FIGURE 13. Unwrapped phase values of virtual antennas according to SNR.

When the SNR was 0 dB, the unwrapped phase formed a straight line, indicating that the phase sequence formed an arithmetic progression. Even when the SNR was −20 dB, which was much lower than the SNR in practical scenarios, the unwrapped phase values showed similar results. On the other hand, there were large errors when the SNR was −40 dB and the angle of the target was not correctly estimated.
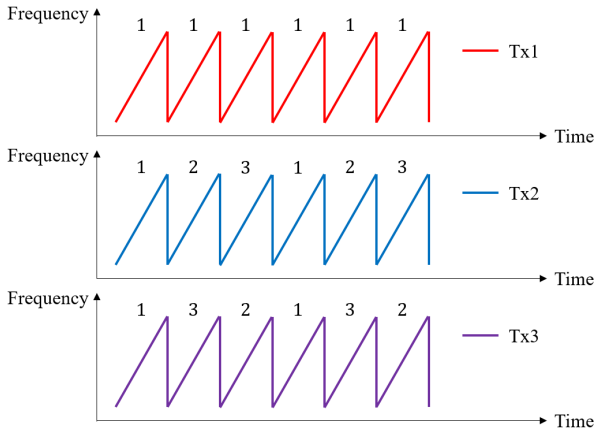
FIGURE 14. Transmitted signals of 3-PSK MIMO radar system (3 Tx antennas).

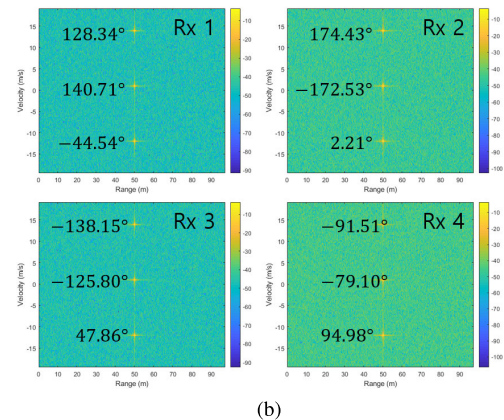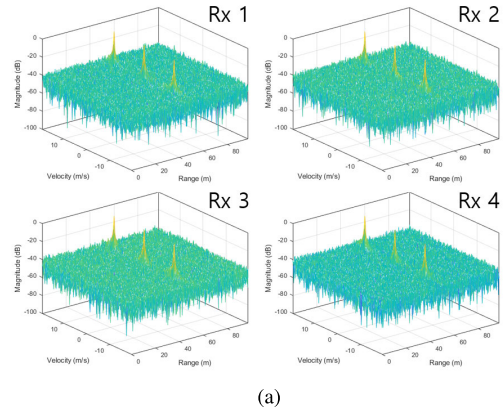**FIGURE 15.** Received signals of 3-PSK MIMO radar system (3 Tx antennas).

FIGURE 16. Range-velocity estimation results of each Rx antenna (3 Tx antennas and 4 Rx antennas): (a) 3D view (b) 2D view from the top.

B. EXPANSION TO M-PSK MIMO SYSTEM

Next, we extend the results for an arbitrary number of Tx antennas. To this end, we use a general phase-shift keying (PSK) modulation scheme in which the phase of the transmitted signals is modulated according to the number of Tx antennas. We will focus on 3 Tx antenna system for simplicity, but the results can be extended to an arbitrary number of Tx antennas. The transmitted signals for a 3-PSK MIMO radar system are shown in Fig. 14. When the chirp is assigned with a code of 1, 2, and 3, the phase of the transmit signal is modulated by 0, $\frac{2\pi}{3}$, and $\frac{4\pi}{3}$, respectively. In other words, the signals

$$s(t)\exp(j0) = \exp\left\{j2\pi\left(f_c t + \frac{B}{2T_c}t^2\right)\right\}, \quad (11)$$

$$s(t)\exp\left(j\frac{2\pi}{3}\right) = \exp\left\{j2\pi\left(f_c t + \frac{B}{2T_c}t^2 + \frac{1}{3}\right)\right\}, \quad (12)$$

$$s(t)\exp\left(j\frac{4\pi}{3}\right) = \exp\left\{j2\pi\left(f_c t + \frac{B}{2T_c}t^2 + \frac{2}{3}\right)\right\} \quad (13)$$

are used. As shown in Fig. 14, Tx 1 transmits with a code of $111111\cdots$, Tx 2 transmits with a code of $123123\cdots$, and Tx 3 transmits with a code of $132132\cdots$. In this case, the received signals can be expressed as Fig. 15, which has a similar structure as shown in Fig. 5. The first term corresponds to the signal transmitted from Tx 1 whose phase increases by $2\pi\frac{2v}{\lambda}T_c$. Moreover, the second and third terms correspond to the signal transmitted from Tx 2 and Tx 3, whose phase increases by $2\pi\frac{2v}{\lambda}T_c + \frac{2\pi}{3}$ and $2\pi\frac{2v}{\lambda}T_c + \frac{4\pi}{3}$, respectively. As a result, when a 2D FFT is applied to the IF band signal, three peaks occur in the range-velocity detection result. One peak corresponds to the true velocity of the target and other two peaks correspond to ghost targets whose velocity is shifted by one-third and two-thirds of the maximum detectable velocity.

Fig. 16 shows the application of the proposed method to the 3-PSK MIMO radar system to solve Doppler-angle ambiguity. We assumed that there are three Tx antennas and

four Rx antennas, where the transmitted signals are modulated according to Fig. 14. In addition, the range, velocity, and angle of the target were set as (50 m, 14 m/s, 15°). As shown in the figure, three peaks occurred due to the properties of 3-PSK modulation. To determine which peak corresponds to which Tx antenna, we performed an arithmetic sequence checking to the obtained phase values. The phase sequence corresponding to the peak location (50 m, −11.97 m/s) was $\boldsymbol{p_a} = [-44.54°\ 2.21°\ 47.86°\ 94.98°]$, those corresponding to the peak location (50 m, 1.01 m/s) was $\boldsymbol{p_b} = [140.71°\ -172.53°\ -125.80°\ -79.10°]$, and those corresponding to the peak location (50 m, 14 m/s) was $\boldsymbol{p_c} = [128.34°\ 174.43°\ -138.15°\ -91.51°]$, respectively.

By arranging these three phase sequences, we note that the cascaded sequence $[\boldsymbol{p_c}\ \boldsymbol{p_a}\ \boldsymbol{p_b}]$ forms an arithmetic progression. Therefore, we can conclude that $\boldsymbol{p_c}$, $\boldsymbol{p_a}$, and $\boldsymbol{p_b}$ correspond to the signal from Tx 1, Tx 2, and Tx 3, respectively. Since the signal from Tx 1 is a general FMCW signal whose phase increases by $2\pi\frac{2v}{\lambda}T_c$, the true velocity of the target can be estimated as 14 m/s. Also, the angle estimation can be performed in a similar manner to Fig. 12 by applying the FFT to the sequence $[\boldsymbol{p_c}\ \boldsymbol{p_a}\ \boldsymbol{p_b}]$. Therefore, the proposed method was effectively applied to 3 Tx antenna system using the 3-PSK modulation scheme and the Doppler-angle ambiguity was resolved.

C. EXPERIMENTAL RESULTS

In this subsection, we verify the performance of the proposed algorithm using the experimental data. We conducted an experiment using the FMCW radar sensor shown in Fig. 17. This FMCW radar supports MIMO mode with two Tx antennas and four Rx antennas, and BPSK modulation can be applied to the transmitted signal. Thus, the system model was equivalent to Fig. 5. In addition, the duration of a chirp which consists of ramp time and idle time was 160 ms, so the maximum detectable velocity was $\pm\frac{\lambda}{4T_c} = \pm6.0392$ m/s. Using this FMCW radar, we collected the data of a corner reflector and a moving person. A photo of the experimental environment is shown in Fig. 18.
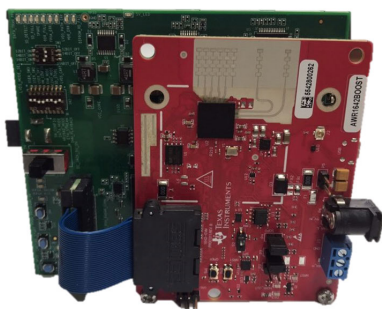

(a)

(b)

FIGURE 18. Photo of experimental environment: (a) corner reflector (b) moving person.

FIGURE 17. AWR1642BOOST radar evaluation board.
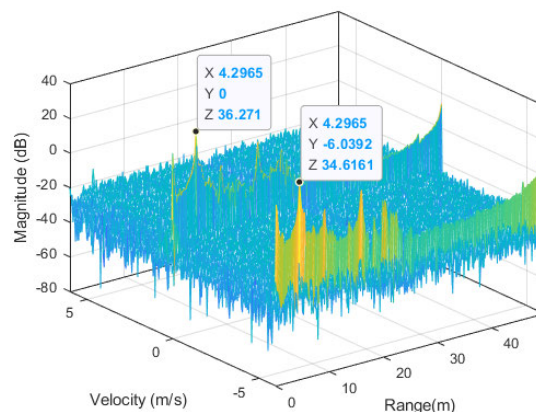
FIGURE 19. Range-velocity estimation result of corner reflector.

First, we present the measurement results of a corner reflector. A corner reflector was placed in front of the radar with a positive angle, meaning that it was placed on the right side of boresight direction. The range-velocity estimation result is shown in Fig. 19. As shown in the figure, one peak occurred at zero velocity, and another peak occurred at -6.0392 m/s which was shifted by half of the maximum detectable velocity. The phase sequence corresponding to the peak location (4.2965 m, -6.0392 m/s) was $\boldsymbol{p_a} = [-77.84°\ -7.03°\ 63.58°\ 144.53°]$ and those corresponding to the peak location (4.2965 m, 0 m/s) was $\boldsymbol{p_b} = [35.53°\ 102.74°\ 167.95°\ -129.28°]$, respectively. Because the cascaded sequence $[\boldsymbol{p_b}\ \boldsymbol{p_a}]$ forms an arithmetic progression, we can decide that 0 m/s is the true velocity of the target. In addition, the angle of the target can be estimated by applying the FFT to the

cascaded sequence $[\boldsymbol{p_b}\ \boldsymbol{p_a}]$. As shown in Fig. 20, the angle of the target was correctly estimated as 21.06°.

Next, we present the measurement results of a moving person. A person was walking in front of the radar with a negative angle, meaning that it was walking on the left side of boresight direction. The range-velocity estimation result is shown in Fig. 21. Unlike the corner reflector which is detected as a point target, a moving person shows the properties of a distributed target since multiple reflections can occur. To clearly identify the reflection from a moving person, we also plotted the result in linear scale. As shown in the figure, one peak occurred at (4.1012 m, -5.3787 m/s) and
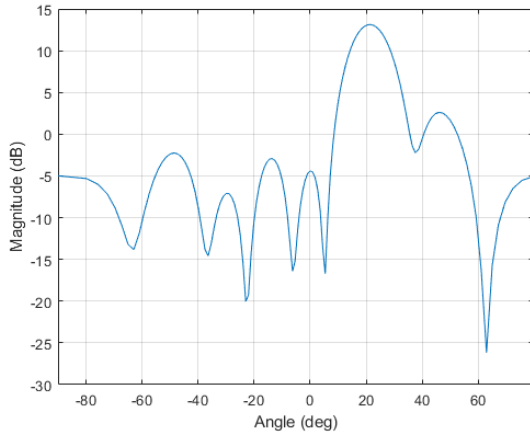
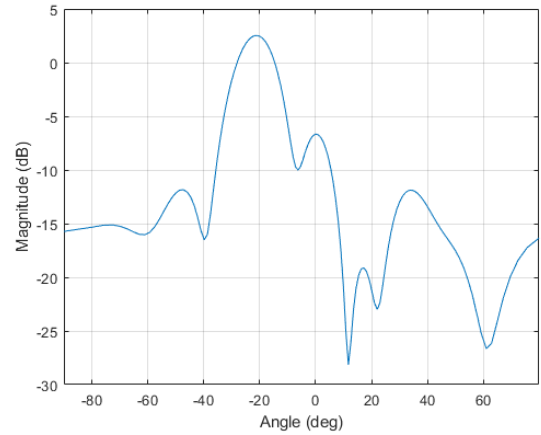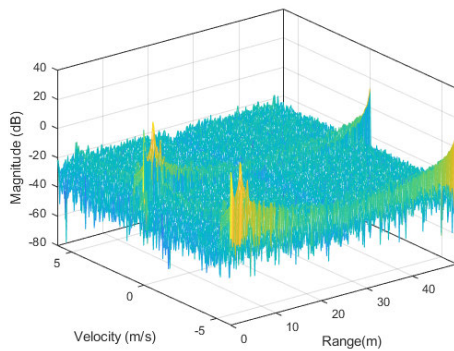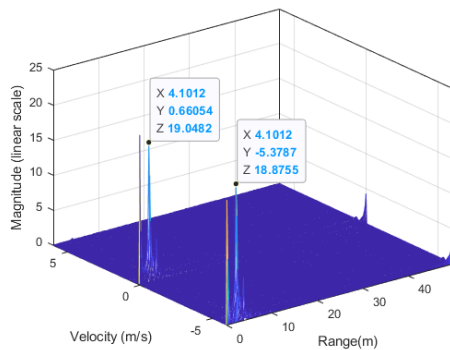**FIGURE 20.** Angle estimation result of corner reflector.

(a)

(b)

FIGURE 21. Range-velocity estimation result of moving person: (a) logarithmic scale (b) linear scale.

another peak occurred at (4.1012 m, 0.66054 m/s). The phase sequence corresponding to the peak location (4.1012 m, -5.3787 m/s) was $\boldsymbol{p}_a = [136.88°\ 73.63°\ 14.82°\ -30.51°]$ and those corresponding to the peak location (4.1012 m, 0.66054 m/s) was $\boldsymbol{p}_b = [50.06°\ -16.98°\ -80.41°\ -145.12°]$, respectively. Because the cascaded sequence $[\boldsymbol{p}_b\ \boldsymbol{p}_a]$ forms an arithmetic progression, we can decide that 0.66054 m/s is the true velocity of the target. In addition, the angle estimation was performed using the cascaded sequence of $[\boldsymbol{p}_b\ \boldsymbol{p}_a]$,

FIGURE 22. Angle estimation result of moving person.

and the angle of $-21.06°$ was correctly estimated as shown in Fig. 22. Using the proposed method, the Doppler-angle ambiguity was resolved and the unambiguous velocity and angle of targets were estimated in both simulated and measured data. Therefore, we believe that the proposed method of modulating the phase of the transmit signals and arranging the phase of the received signals to distinguish signals from each Tx antenna will help to improve the performance of MIMO radar systems.

V. CONCLUSION
In the BPSK-MIMO FMCW radar system, the estimated range and velocity values corresponding to each target are duplicated as many as the number of Tx antennas, and they are detected as ghost targets. Thus, a method for solving the Doppler-angle ambiguity in the BPSK-MIMO FMCW radar system was proposed. The result of range-velocity detection of each Rx antenna showed that the phase values of signals corresponding to the same target should have the form of an arithmetic sequence. Based on this observation, we solved the Doppler ambiguity by correctly arranging the phase values derived from each target. The performance of the proposed method was evaluated with both simulated and measured data. The maximum detectable velocity was maintained using the proposed method even when multiple Tx antennas were used. Moreover, inaccuracies in angle estimation due to the movement of the target was resolved.

REFERENCES
[1] E. Fishler, A. Haimovich, R. Blum, D. Chizhik, L. Cimini, and R. Valenzuela, "MIMO radar: An idea whose time has come," in *Proc. IEEE Radar Conf.*, Philadelphia, PA, USA, Apr. 2004, pp. 71–78.

[2] H. Sun, F. Brigui, and M. Lesturgie, "Analysis and comparison of MIMO radar waveforms," in *Proc. Int. Radar Conf.*, Lille, France, Oct. 2014, pp. 1–6.

[3] J. J. M. de Wit, W. L. van Rossum, and A. J. de Jong, "Orthogonal waveforms for FMCW MIMO radar," in *Proc. IEEE Radar Conf.*, Kansas City, MO, USA, May 2011, pp. 686–691.

[4] A. Zwanetski and H. Rohling, "Continuous wave MIMO radar based on time division multiplexing," in *Proc. 13th Int. Radar Symp.*, Warsaw, Poland, May 2012, pp. 119–121.

[5] F. Belfiori, N. Maas, P. Hoogeboom, and W. van Rossum, "TDMA X-band FMCW MIMO radar for short range surveillance applications," in *Proc. Eur. Conf. Antennas Propag.*, Rome, Italy, 2011, pp. 483–487.

[6] B. Liu, "Orthogonal discrete frequency-coding waveform set design with minimized autocorrelation sidelobes," *IEEE Trans. Aerosp. Electron. Syst.*, vol. 45, no. 4, pp. 1650–1657, Oct. 2009.

[7] R. Feger, C. Pfeffer, and A. Stelzer, "A frequency-division MIMO FMCW radar system using delta-sigma-based transmitters," in *IEEE MTT-S Int. Microw. Symp. Dig.*, Tampa, FL, USA, Jun. 2014, pp. 1–4.

[8] H. He, P. Stoica, and J. Li, "Designing unimodular sequence sets with good correlations—Including an application to MIMO radar," *IEEE Trans. Signal Process.*, vol. 57, no. 11, pp. 4391–4405, Nov. 2009.

[9] M. Mbeutcha and V. Krozer, "CDMA-based MIMO FMCW radar system performance using intra-pulse phase modulation," in *Proc. Eur. Radar Conf.*, Paris, France, 2019, pp. 233–236.

[10] F. Roos, J. Bechter, N. Appenrodt, J. Dickmann, and C. Waldschmidt, "Enhancement of Doppler unambiguity for chirp-sequence modulated TDM-MIMO radars," in *IEEE MTT-S Int. Microw. Symp. Dig.*, Munich, Germany, Apr. 2018, pp. 1–4.

[11] C. M. Schmid, R. Feger, C. Pfeffer, and A. Stelzer, "Motion compensation and efficient array design for TDMA FMCW MIMO radar systems," in *Proc. 6th Eur. Conf. Antennas Propag. (EUCAP)*, Prague, Czech Republic, Mar. 2012, pp. 1746–1750.

[12] K. Rambach and B. Yang, "Colocated MIMO radar: cramer-rao bound and optimal time division multiplexing for DOA estimation of moving targets," in *Proc. IEEE Int. Conf. Acoust., Speech Signal Process.*, Vancouver, BC, Canada, May 2013, pp. 4006–4010.

[13] K. Thurn, D. Shmakov, G. Li, S. Max, M.-M. Meinecke, and M. Vossiek, "Concept and implementation of a PLL-controlled interlaced chirp sequence radar for optimized range–Doppler measurements," *IEEE Trans. Microw. Theory Techn.*, vol. 64, no. 10, pp. 3280–3289, Oct. 2016.

[14] Y. Li, C. Xu, X. Yan, and Q. Liu, "An improved algorithm for Doppler ambiguity resolution using multiple pulse repetition frequencies," in *Proc. 9th Int. Conf. Wireless Commun. Signal Process. (WCSP)*, Nanjing, China, Oct. 2017, pp. 1–5.

[15] Y. L. Sit, G. Li, S. Manchala, H. Afrasiabi, C. Sturm, and U. Lubbert, "BPSK-based MIMO FMCW automotive-radar concept for 3D position measurement," in *Proc. 15th Eur. Radar Conf. (EuRAD)*, Madrid, Spain, Sep. 2018, pp. 289–292.

[16] R. Y. Chiao, L. J. Thomas, and S. D. Silverstein, "Sparse array imaging with spatially-encoded transmits," in *Proc. IEEE Ultrason. Symp. Proc.*, Toronto, ON, Canada, Oct. 1997, pp. 1679–1682.

[17] H. A. Gonzalez, C. Liu, B. Vogginger, and C. G. Mayr, "Doppler ambiguity resolution for binary-phase-modulated MIMO FMCW radars," in *Proc. Int. Radar Conf. (RADAR)*, Toulon, France, Sep. 2019, pp. 1–6.

[18] Z. T. Ziqiang Tong, R. Reuter, and M. Fujimoto, "Fast chirp FMCW radar in automotive applications," in *Proc. IET Int. Radar Conf.*, Hangzhou, China, 2015, pp. 1–4.

[19] S. M. Patole, M. Torlak, D. Wang, and M. Ali, "Automotive radars: A review of signal processing techniques," *IEEE Signal Process. Mag.*, vol. 34, no. 2, pp. 22–35, Mar. 2017.

[20] S. Tahcfulloh and G. Hendrantoro, "Phased-MIMO radar using Hadamard coded signal," in *Proc. Int. Conf. Radar, Antenna, Microw., Electron., Telecommun. (ICRAMET)*, Jakarta, Indonesia, Oct. 2016, pp. 13–16.

[21] R. O. Schmidt, "Multiple emitter location and signal parameter estimation," *IEEE Trans. Antennas Propag.*, vol. AP-34, no. 3, pp. 276–280, Mar. 1986.

[22] R. Roy and T. Kailath, "Esprit-estimation of signal parameters via rotational invariance techniques," *IEEE Trans. Acoust., Speech, Signal Process.*, vol. 37, no. 7, pp. 984–995, Jul. 1989.

[23] M. A. Richards, "Constant false alarm rate (CFAR) detection," in *Fundamentals of Radar Signal Processing*. New York, NY, USA: McGraw-Hill, 2001, pp. 347–383.

JAEHOON JUNG (Graduate Student Member, IEEE) received the B.S. degree in electrical and computer engineering from Seoul National University, Seoul, Republic of Korea, in 2018, where he is currently pursuing the Ph.D. degree. His research interests include radar signal processing techniques, especially on automotive radar systems.

SOHEE LIM (Graduate Student Member, IEEE) received the B.S. degree in electrical and computer engineering from Seoul National University, Seoul, South Korea, in 2017, where she is currently pursuing the Ph.D. degree. Her research interests include radar signal processing techniques, including automotive radar and UWB radar, particularly on clutter and interference suppression, and target detection and classification.

SEONG-CHEOL KIM (Senior Member, IEEE) received the B.S. and M.S. degrees from Seoul National University, Seoul, South Korea, in 1984 and 1987, respectively, and the Ph.D. degree from the Polytechnic Institute of NYU, Brooklyn, NY, USA, in 1995, all in electrical engineering. From 1995 to 1999, he was with Wireless Communications Systems Engineering Department, AT&T Bell Laboratories, Holmdel, NJ, USA. Since 1999, he has been a Professor with the Department of Electrical and Computer Engineering, Seoul National University. His current research interests include wireless communication systems, including millimeter wave channel modeling, wireless localization algorithms, power line communications, and automotive radar signal processing techniques.

SEONGWOOK LEE (Member, IEEE) received the B.S. and Ph.D. degrees in electrical and computer engineering from Seoul National University (SNU), Seoul, Republic of Korea, in February 2013 and August 2018, respectively. From September 2018 to February 2020, he worked as a Staff Researcher at Machine Learning Laboratory, AI & SW Research Center, Samsung Advanced Institute of Technology (SAIT), Suwon-si, Gyeonggi-do, Republic of Korea. Since March 2020, he has been an Assistant Professor with the School of Electronics and Information Engineering, College of Engineering, Korea Aerospace University, Goyang-si, Gyeonggi-do, South Korea. He has published more than 60 papers on radar signal processing. His research interests include automotive radar signal processing techniques, such as enhanced target detection and tracking, target recognition and classification, clutter suppression and mutual interference mitigation, and multiple-input multiple-output radar and synthetic aperture radar imaging. He received the Distinguished Ph.D. Dissertation Award from the Department of Electrical and Computer Engineering, SNU.

● ● ●